RSC Advances

This is an *Accepted Manuscript*, which has been through the Royal Society of Chemistry peer review process and has been accepted for publication.

Accepted Manuscripts are published online shortly after acceptance, before technical editing, formatting and proof reading. Using this free service, authors can make their results available to the community, in citable form, before we publish the edited article. This *Accepted Manuscript* will be replaced by the edited, formatted and paginated article as soon as this is available.

You can find more information about *Accepted Manuscripts* in the Information for Authors.

Please note that technical editing may introduce minor changes to the text and/or graphics, which may alter content. The journal's standard Terms & Conditions and the Ethical guidelines still apply. In no event shall the Royal Society of Chemistry be held responsible for any errors or omissions in this *Accepted Manuscript* or any consequences arising from the use of any information it contains.

ROYAL SOCIETY OF CHEMISTRY

www.rsc.org/advances

Cite this: DOI: 10.1039/c0xx00000x

www.rsc.org/xxxxxx

ARTICLE TYPE

Investigation of the porosity of atomic layer deposited ultra-thin Al_2O_3 films by using electrochemical measurement

Zhimin Chai,[a] Jing Li,[ab] Xinchun Lu*[a] and Dannong He[c]

Received (in XXX, XXX) Xth XXXXXXXXX 20XX, Accepted Xth XXXXXXXXX 20XX
DOI: 10.1039/b000000x

The porosity of ultra-thin alumina (Al_2O_3) films was measured by electrochemical experiment. The Al_2O_3 films were prepared by atomic layer deposition (ALD) on a copper substrate using trimethyl aluminum (TMA) and water as precursors. The copper substrate was fine polished to decrease the influence of surface defects on porosity. 30 to 300 ALD cycles were conducted to get films with a thickness in a range of 4.5 to 29.4 nm. The Auger electron spectroscopy (AES) result reveals that the Al_2O_3 films prepared by ALD are well stoichiometric and that the Al_2O_3 films show less substrate sensitivity. The results obtained by potentiodynamic polarization demonstrate that the porosity of the Al_2O_3 films decreases with the film thickness. However, when the film thickness increases to 7.8 nm, the film porosity tends to become stable. With further increasing film thickness, the porosity decreases rather slowly. Because of the low porosity of the 7.8 nm Al_2O_3 film, the copper substrate is well protected. No obvious corrosion can be observed in the scanning electron microscopy (SEM) images.

Keywords: porosity, ALD, Al_2O_3, potentiodynamic polarization

1. Introduction

Nowadays, films as a good alternative to bulk materials are widely used in micro device applications. As the size of micro devices continues to shrink, the film thickness is progressively driven to its extremity. To name a few, in complementary metal oxide semiconductors (CMOS) and dynamic random access memory (DRAM) applications, high dielectric constant (high-*k*) oxide films with a thickness <10 nm are used to provide sufficient capacitance.[1-3] As the feature size of integrated circuits (IC) scaled down to sub-32 nm, a diffusion barrier with a thickness <5 nm is required to prevent copper from diffusing into low-*k* materials.[4] And in order to increase the magnetic storage density over 1 Tbit/in.[2], the thickness of protective diamond like carbon (DLC) films should be as thin as 1-2 nm.[5, 6] With the continuing shrinking of film thickness to several nanometers, the film may be discontinuous and massive pinhole defects formed in the initial period of film growth remain in the film, which would lead to failure of many devices. Therefore, the knowledge of a critical thickness at which films become continuous and compact has great significance for the normal operation of many devices.

Alumina (Al_2O_3) is a technologically important material due to its excellent insulation properties, high chemical and thermal stabilities, high mechanical strength and high corrosion resistance.[7] Because of these properties, Al_2O_3 films are widely used in micro devices as high *k* dielectric layers,[1-3, 8] diffusion barrier layers,[4, 9-12] and protective coatings. Ultra-thin Al_2O_3 films can be deposited by an atomic layer deposition (ALD) process.[13, 14] In the ALD process, two precursor gases are pulsed onto a substrate surface alternately and between the precursor pulses, the reaction chamber is purged with an inert gas. The self-limiting growth mechanism of the ALD process enables a precision thickness to be controlled at a monolayer level. Moreover, excellent step coverage, conformal deposition on high aspect ratio structures, nearly pinhole free and uniform composition control are also well ensured.

Electrochemical measurements (linear scan voltammetry (LSV) and electrochemical impedance spectroscopy (EIS)) have been used to get the porosity of ultra-thin Al_2O_3 films grown by thermal ALD.[15-17] However, because of polishing scratches and particle contaminations existing on substrate surface, the resulting porosity of ultra-thin Al_2O_3 films may be overestimated.[18, 19] H_2–Ar plasma pre-treatment has been employed to remove the organic contamination of the substrate.[20, 21] After pre-treatment, the influence of substrate on the porosity was eliminated to some extent and the film porosity decreased by 1–3 orders of magnitude. However, the influence of scratch on the substrate surface on the porosity still exists, thus, how to eliminate the influence is the concern of this study.

In the present study, potentiodynamic polarization measurement was employed to obtain the porosity of ultra-thin Al_2O_3 films prepared by ALD on a copper substrate. Based on the analysis of films with a thickness from 4.5 to 29.4 nm, the critical thickness at which film became continuous and compact was ultimately found. Because defects and contaminations on the surface of the copper substrate would give rise to the failure of the Al_2O_3 films as indicated above, the copper substrate was fine polished to decrease the surface defects.

RSC Advances Accepted Manuscript

2. Experimental methods

2.1. Surface preparation

A copper sample (99.99 wt% purity) with sizes of 20 × 20 × 2 mm^3 was used as the substrate to grow ultra-thin Al_2O_3 films. Firstly, the copper substrate was mechanically polished using a TegraPol instrument (Struers) with silicon carbide (SiC) foils (Grit size #320, #500 and #1200) as grinding mediums. Then chemical mechanical polishing (CMP) was conducted to further decrease the surface roughness. Commercial slurry (PL-7105, Fujimi) consisting of chemical reagents and submicron sized abrasive particles was used in the CMP process. Prior to use, the slurry was diluted by deionized water with a dilution ratio of 1:3. Finally, the substrate was cleaned in an ultrasonic deionized water bath for 2 min and then blow-dried with a pure nitrogen (99.99%).

2.2. Films prepared by atomic layer deposition

Al_2O_3 films were deposited on the copper substrate using a Picosun SUNALE R-150 ALD reactor. The precursors employed were trimethyl aluminum (purity >99.99%) and water which were kept at room temperature.[14, 22] These two precursors were alternately pulsed into a reaction chamber with a high purity nitrogen (purity >99.999%) as a carrier gas. Between the precursor pulses, the reaction chamber was purged with the high purity nitrogen. The flow rates of the carrier gas and purge gas were both 150 sccm. One complete ALD cycle consisted of 0.1 s of TMA/N_2, 3 s of N_2, 0.1 s of H_2O/N_2, and 4 s of N_2. Long purge time was adopted in order to prevent the reaction of two precursors. By adjusting the number of ALD cycles, ultra-thin Al_2O_3 films with various thicknesses were obtained. During deposition, the pressure in the chamber was kept ~14 hPa by a dry pump, and the temperature in the chamber was limited to 150 °C to avoid the oxidization of copper substrate. After preparation, the samples were kept in a vacuum drier.

The thickness of the Al_2O_3 films was measured from silicon wafer which was coated simultaneously with the copper substrate. Before deposition, a Si (100) substrate was cleaned in ultrasonic acetone, absolute alcohol and deionized water baths for 10 min, respectively. The film thickness was measured by a null-ellipsometry (Multiskop, Optrel) under the ambient air. The wavelength of the Nd-YAG laser was 632.8 nm and the incidence was 70°. Modeling was performed using the Elli software (Optrel). A 2-layer model (air/substrate) was used to determine the refractive index and absorption coefficient of the substrate. The thickness of the Al_2O_3 films was then calculated using a 3-layer model (air/film/substrate).

Because the thickness of the Al_2O_3 films was measured from the Si (100) substrate, a question arises as to whether the thickness values measured were consistent with that measured from the copper substrate. To make clear this question, elemental depth profiles were obtained for Al_2O_3 film coated Si (100) and copper substrates, respectively, using an Auger electron spectroscopy (AES, PHI-700, ULVAC-PHI) with a co-axial cylindrical mirror analyzer (CMA). The spectrometer was operated at a pressure of $<3.9\times10^{-9}$ Torr. The depth profiling was done with a 5 kV Ar ion sputter beam at an incident angle of 30°. The sputtering rate of a SiO_2 film (calibration specimen) was 6 nm/min.

2.3. Electrochemical measurements

The electrochemical measurements were carried out with an M237A potentiostat (EG&G) with a three-electrode cell. A platinum wire was used as counter electrode, and silver/silver chloride (Ag/AgCl) electrode as reference electrode. The area of working electrode was restricted to 2.01 cm^2 by an O-ring. The electrolyte solution was 0.1 M NaCl prepared by ultra-pure water (resistivity >18 MΩcm) and reagent grade chemicals (NaCl Analar Normapur analytical reagent, Sinopharm Chemical Reagent Co). Before the electrochemical measurements, the open circuit potential (OCP) was stabilized for 30 min. Then, the electrochemical polarization tests were performed with a scan rate of 2 mV/s from −0.25 V up to 0.3 V with respect to OCP.

2.4. Porosity evaluation

Figure 1 shows the diagram of Al_2O_3 film coated copper system immersed in the 0.1 M NaCl solution. Pinhole defects appear in the Al_2O_3 film. At these sites, NaCl solution can permeate the film and reach the copper substrate. Therefore, corrosion of substrate occurs. By comparing the corrosion of the copper substrate before and after coated with the Al_2O_3 film, the porosity of the Al_2O_3 film can be quantitatively measured. Several methods have been adopted to calculate the porosity of the film.[15, 21, 23-25] In our study, the comparison of the polarization resistances of uncoated and coated samples was used:[25]

$$P=\frac{R_{\mathrm{ps}}}{R_{\mathrm{p}}}\times10^{-|\Delta E_{\mathrm{corr}}|/b_{\mathrm{a}}}, \qquad (1)$$

where P is the porosity of the Al_2O_3 film, R_{ps} is the polarization resistance of the copper substrate, R_p is the polarization resistance of the Al_2O_3 film coated copper, ΔE_{corr} is the difference in free corrosion potentials between the coated copper and bare copper substrate, and ba is the anodic Tafel slope of the copper substrate. The corrosion potential E_{corr}, corrosion current density i_{corr}, anodic Tafel slope ba and cathodic Tafel slope bc can be obtained by the Tafel extrapolation method from polarization curves.[26] Tafel lines are obtained from the linear portion of the polarization curves, and the corrosion current density is obtained from the intersection of the Tafel lines at the corrosion potential. Then the polarization resistance is obtained using the Stern–Geary equation:[27]

$$R_{\mathrm{p}}=\frac{b_{\mathrm{a}}b_{c}/\left[2.303\left(b_{\mathrm{a}}+b_{c}\right)\right]}{i_{\mathrm{corr}}}. \qquad (2)$$

This journal is © The Royal Society of Chemistry [year]

RSC Advances Accepted Manuscript

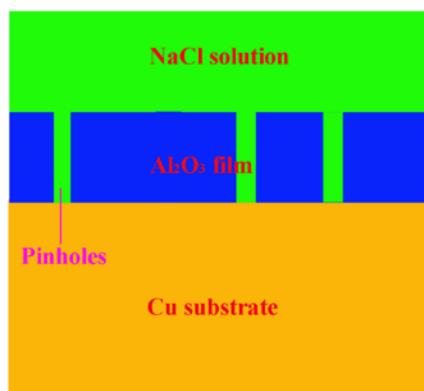

Figure 1. Diagram of Al_2O_3 film coated copper system immersed in the 0.1 M NaCl solution.

2.5 Surface analysis

The surface morphologies of samples before and after electrochemical measurements were observed using an atomic force microscope (AFM, Veeco) and a scanning electron microscopy (SEM, FEI Quanta 200 FEG) operating at a 20 kV accelerating voltage. The composition of the corroded copper surface was determined by a X-ray photoelectron spectroscopy (XPS, PHI Quantera SXM). The binding energy was calibrated by taking the carbon C1s peak (284.8 eV) as reference.

3. Results and discussion

3.1 Substrate surface

Figure 2 (a) shows the SEM image of the surface of the polished copper substrate. Unlike the substrates used in a previous literature,[17] the copper substrate reveals no obvious defects, which can reduce the influence of the surface defects on the film porosity. The grain boundary of the polycrystalline copper substrate is visual even though it is not clear. Figure 2 (b) shows a AFM image of the polished copper substrate. The surface of the copper substrate is very smooth, and the root-mean-square (RMS) roughness of the surface is 0.72 nm. Because of the high z-resolution of the AFM, the grain boundary can be clearly seen. Figure 2 (c) is a cross sectional profile of the copper substrate indicated in (b) as a blue line. The segment between two green dashed lines (two green crosses in (b)) is the grain boundary. It can be seen that the depth of the grain boundary is ~2 nm. That explains why the grain boundary cannot be seen clearly by the SEM.

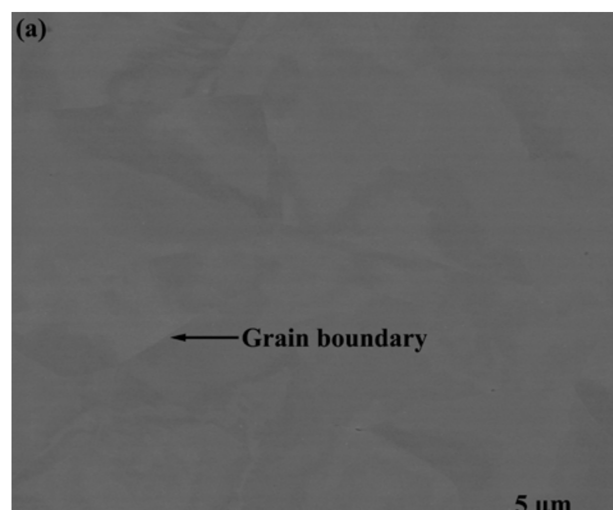

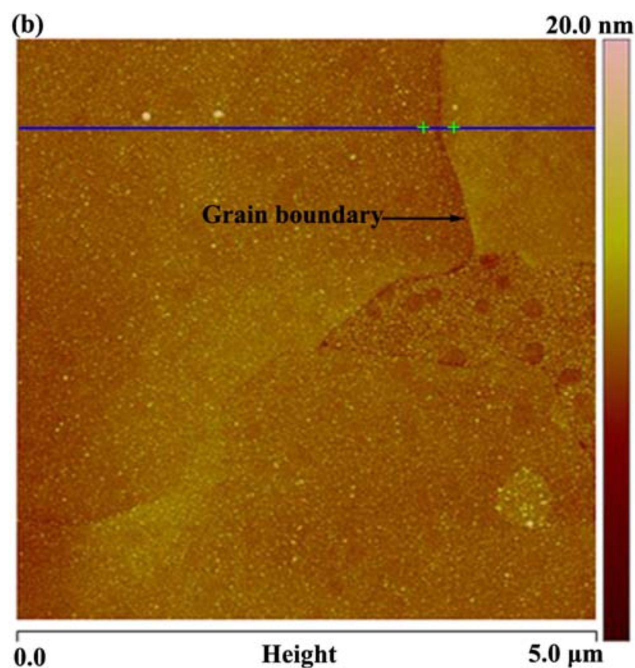

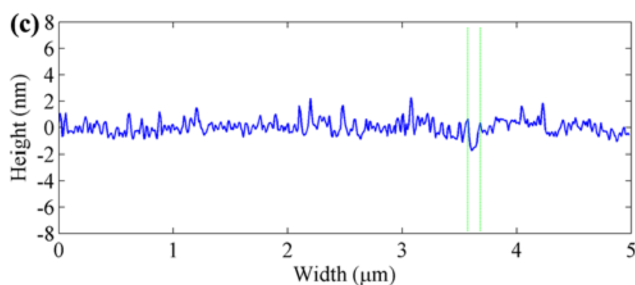

Figure 2. (a) SEM image of the polished copper substrate. Black arrow: grain boundary. (b) AFM image of the polished copper substrate. Black arrow: grain boundary. (c) Cross sectional profile of the copper substrate indicated in (b) as a blue line, and the segment between two green dashed lines is the grain boundary.

3.2 Film thickness

The growth behavior of the ALD Al_2O_3 films was investigated by the ellipsometry. 30-300 ALD cycles were preformed to get the ultra-thin Al_2O_3 films with different thicknesses. Figure 3 shows

RSC Advances Accepted Manuscript

the film thickness of Al_2O_3 as a function of the number of ALD cycles. Each value in the figure is an average of 6 points measured at different locations of the sample. The film thicknesses were almost linear with respect to the number of ALD cycles, which indicates the self-limiting growth mechanism of the ALD process.

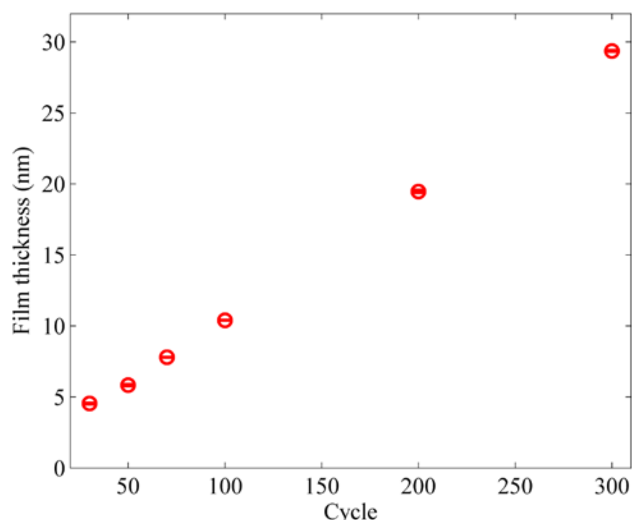

Figure 3. The thickness of the Al_2O_3 films as a function of number of ALD cycles.

AES was used to determine whether the Al_2O_3 films deposited on the Si (100) substrate have the same thickness with that deposited on the copper substrate. Figure 4 (a) and (b) show the depth profiles of the Al_2O_3 films deposited with 200 ALD cycles on the copper and Si (100) substrates, respectively. Due to the exposure to the ambient air, a high concentration of C element can be observed on the very surface of the Al_2O_3 film. For the Al_2O_3 films deposited on both substrates, plateaus of the O and Al elements are observed, which indicates that the films have a uniform in-depth stoichiometry. Moreover, for both samples, the concentrations of Al and O decrease after about 4.5 min of sputtering, which demonstrates that the two Al_2O_3 films deposited on the copper and Si (100) substrates have the same film thickness.

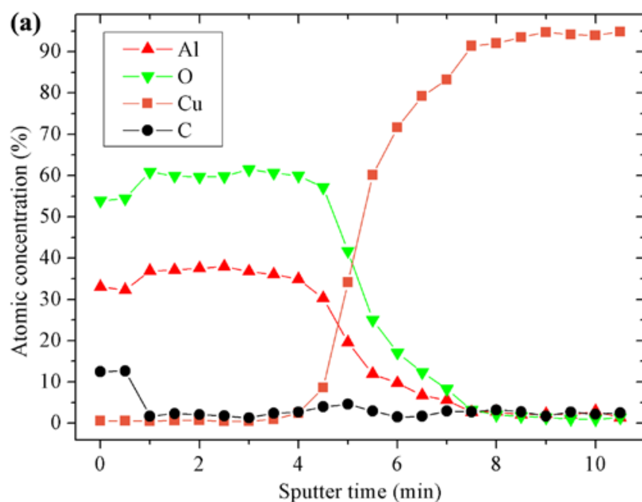

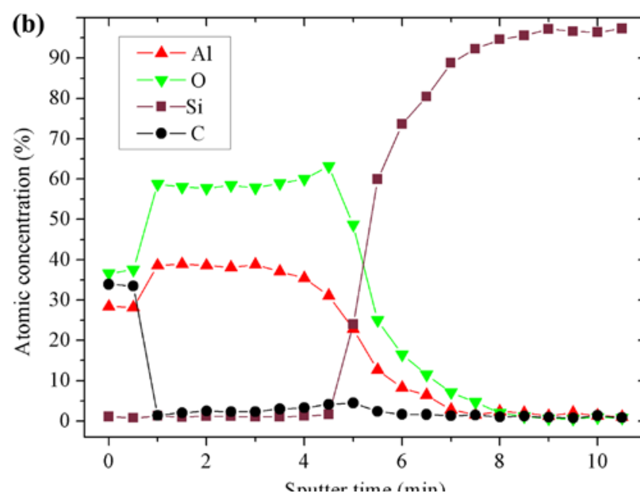

Figure 4. Depth profiles of the Al_2O_3 film deposited with 200 ALD cycles on (a) the copper and (b) the Si (100) substrates, respectively.

3.3 Electrochemical polarization

Figure 5 (a) shows the polarization curves of the copper substrate and Al_2O_3 film coated samples. Several electrochemical parameters, such as corrosion potential (E_{corr}), corrosion current density (i_{corr}), anodic Tafel slope (b_a) and cathodic Tafel slope (b_c), are deduced from the polarization curves, as listed in Table 1. The corrosion potential of the bare substrate is -0.113 V (Ag/AgCl). However, for the coated samples, corrosion potentials shifted anodically. With the increase of Al_2O_3 film thickness, the corrosion potential becomes more anodic, which shows an enhanced corrosion resistance. The corrosion current densities of Al_2O_3 film coated samples are significantly smaller than that of the copper substrate, and with the increase of film thickness from 4.5 nm to 7.8 nm, the corrosion current densities of Al_2O_3 film coated samples reduce by 1 orders of magnitude. When the thickness of the Al_2O_3 films further increases, the corrosion current tends to become stable.

The corrosion resistance of the Al_2O_3 film coated samples is related to the film porosity. The porosity of Al_2O_3 film coated samples is obtained from Eq. (1), where the polarization resistances (R_p) is calculated from Eq. (2) using electrochemical parameters listed in Table 1. The porosity of the Al_2O_3 film coated samples as a function of film thickness is shown in Figure 5 (b). It can be seen that the porosity of the Al_2O_3 film coated samples decreases with the increase of film thickness, which explains the decrease of corrosion current density with film thickness. The decreased porosity of the Al_2O_3 films is assigned to the progressively sealed defects formed in the initial period of film growth. The porosity of a 7.8 nm thick Al_2O_3 film is 2.86%. With further increasing film thickness, the porosity tends to become stable. Accordingly, the corrosion current density of the Al_2O_3 film coated samples becomes stable.

It should be mentioned that the porosities of the Al_2O_3 films with thickness of 5.9 nm and 10.4 nm are 15.53% and 1.74%, much lower than previous reported 35.48% (5 nm thick Al_2O_3 film) and 31.45% (10 nm thick Al_2O_3 film).[16] Low film porosity can be assigned to the reduced surface defects of the copper substrate. In our study, the copper substrate was fine polished to decrease the surface defect densities, which enables the Al_2O_3

This journal is © The Royal Society of Chemistry [year]
RSC Advances Accepted Manuscript

films to nucleate uniformly on the surface of the copper substrate. As the influence of surface defects on the growth of the Al_2O_3 films is eliminated in our study, the measured porosities can be more accurate.

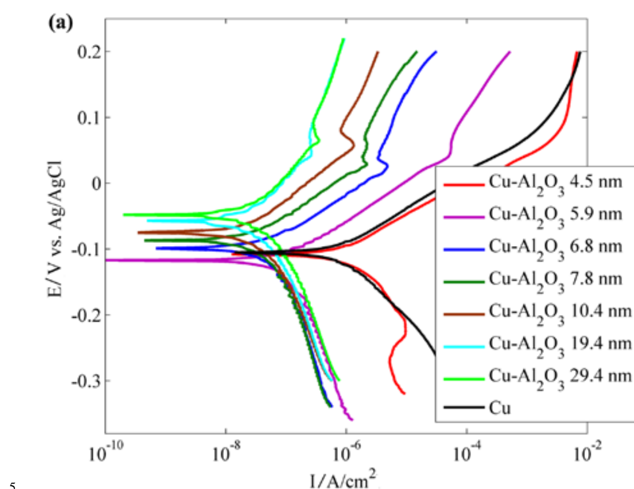

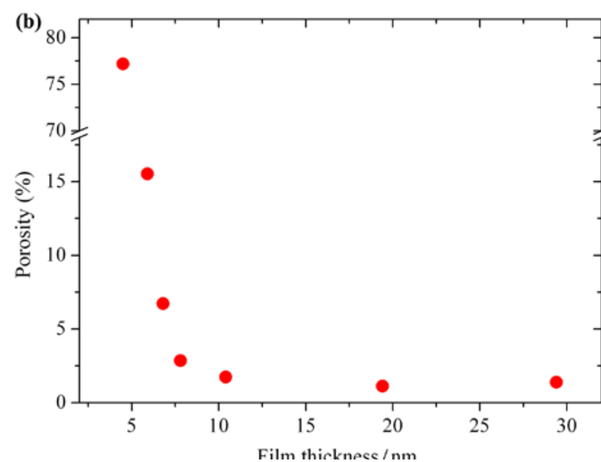

Figure 5. (a) Polarization curves for the copper substrate and Al_2O_3 film coated samples in 0.1 M NaCl solution; (b) The porosities of Al_2O_3 film coated samples.

Table 1. Electrochemical polarization data of copper substrate and Al_2O_3 film coated samples.

Samples	E_{corr} (V)	i_{corr} (A/cm^2)	b_a (V/dec)	b_c (V/dec)	R_p (Ωcm^2)
Cu	-0.113	5.37e-007	0.148	0.065	3.66e+004
4.5 nm Al_2O_3	-0.108	3.19e-007	0.042	0.132	4.38e+004
5.9 nm Al_2O_3	-0.117	1.15e-007	0.062	0.165	2.21e+005
6.8 nm Al_2O_3	-0.099	4.33e-008	0.060	0.162	4.37e+005
7.8 nm Al_2O_3	-0.087	2.29e-008	0.059	0.184	8.54e+005
10.4 nm Al_2O_3	-0.075	1.80e-008	0.069	0.157	1.16e+006
19.4 nm Al_2O_3	-0.057	1.59e-008	0.076	0.141	1.35e+006
29.4 nm Al_2O_3	-0.048	2.99e-008	0.111	0.164	9.60e+005

Figure 6 (a) and (b) show the SEM images of the copper substrate after corrosion. The copper substrate corrodes severely, and a large amount of bamboo-like structures appear on the copper surface. Similar structures have been observed in a previous literature.[28] The copper substrate is corroded uniformly because bamboo-like structures are distributed uniformly. Figure 7 (a), (b) and (c) show the XPS spectra of Cu 2p, O 1s and Cl 2p core levels of the corroded copper substrate, respectively. The peak position of the Cu 2p core level appears at 932.8 eV, which may be ascribed to the presence of CuCl or Cu_2O.[29-31] These two matters cannot be distinguished from one another because of their close binding energy. The O 1s peak at 530.8 eV is due to the presence of the Cu_2O,[29] and the Cl 2p peaks at 198.9 eV and 200.5 eV are due to the presence of the CuCl.[31] The existence of O 1s and Cl 2p peaks demonstrates that both CuCl and Cu_2O are formed during the corrosion process. Overall reaction of copper in NaCl solution is as followed:[32]

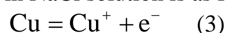
$$Cu = Cu^+ + e^- \quad (3)$$

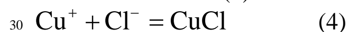
$$Cu^+ + Cl^- = CuCl \quad (4)$$

$$2CuCl + H_2O = Cu_2O + 2H^+ + 2Cl^- \quad (5)$$

Figure 6 (c) and (d) display the images of the copper substrate coated with a 4.5 nm thick Al_2O_3 film after corrosion. Due to the large porosity of the 4.5 nm Al_2O_3 film, bamboo-like structures can also be observed, but the amount of bamboo-like structures is decreasing. Figure 6 (e) and (f) show the images of the 7.8 nm Al_2O_3 film coated copper substrate after corrosion. Because of the low porosity of the 7.8 nm Al_2O_3 film, the copper substrate is well protected. Only local corrosion occurs, which reveal as spots existing on the image. The local corrosion behavior confirms the fact that the corrosion is caused by pinhole defects.

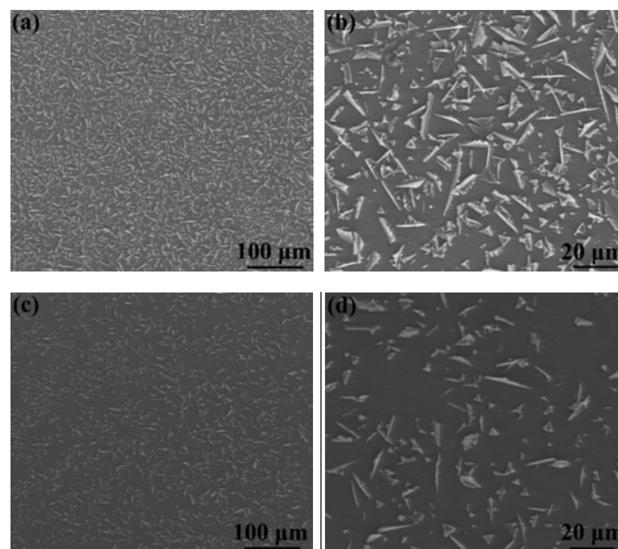

RSC Advances Accepted Manuscript

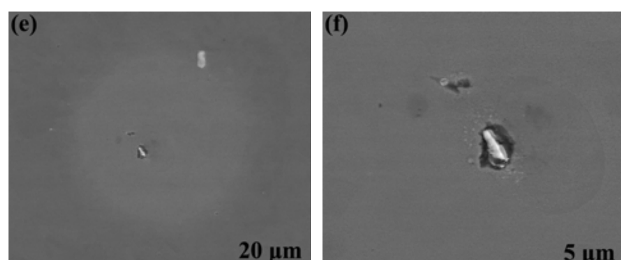

Figure 6. (a) SEM image of the copper substrate after electrochemical polarization measurement. (b) A magnified image of (a). (c) SEM image of the 4.5 nm Al_2O_3 film coated copper substrate after electrochemical polarization measurement. (d) A magnified image of (c). (e) SEM image of the 7.8 nm Al_2O_3 film coated copper substrate after electrochemical polarization measurement. (f) A magnified image of (e).

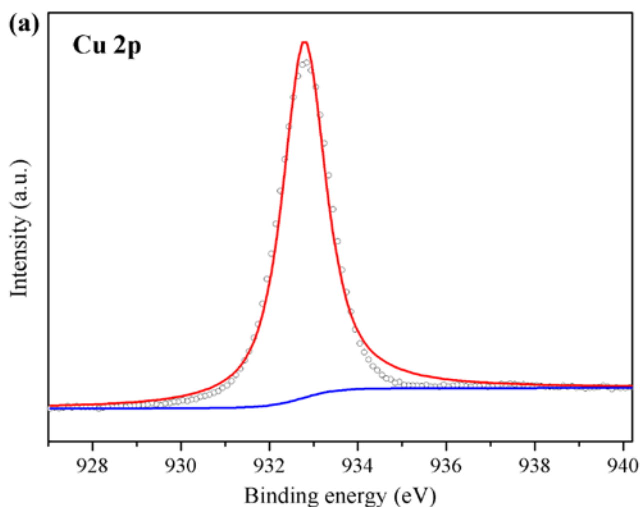

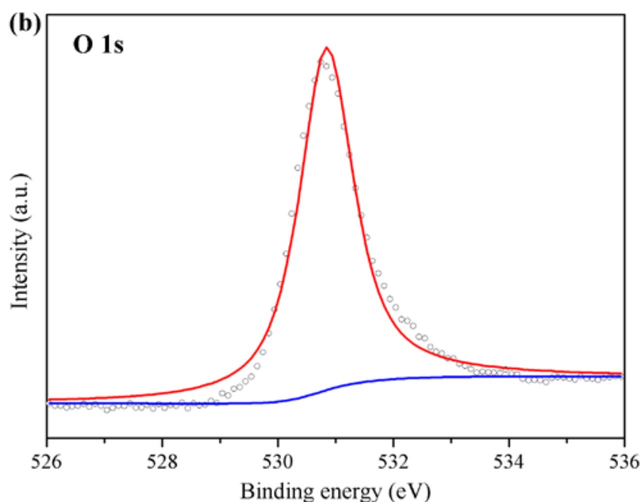

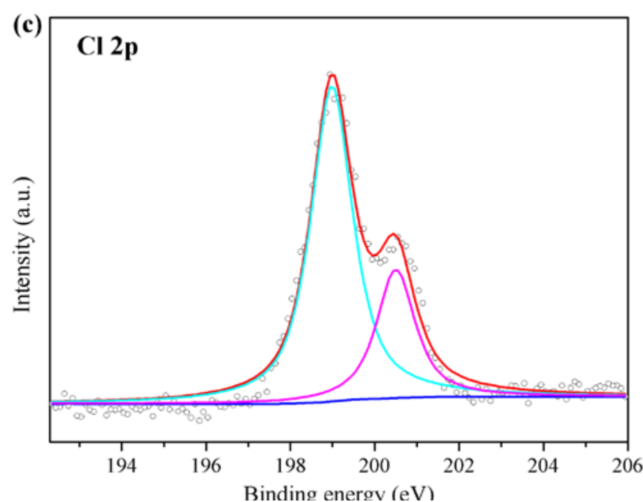

Figure 7. XPS spectra of (a) Cu 2p, (b) O 1s and (c) Cl 2p core levels of the corroded copper substrate

4. Conclusions

Electrochemical measurements were performed to get the porosity of the ultra-thin Al_2O_3 films prepared by ALD. Because the surface of the copper substrate was fine polished, the influence of surface defects on the film porosity was eliminated to some extent, and the resulting porosity values are smaller than those in previous studies. The AES results demonstrate that the Al_2O_3 films are well stoichiometric, and that the Al_2O_3 films deposited on the copper substrate have the same thickness with that deposited on the Si (100) substrate. The porosity of the Al_2O_3 films obtained from potentiodynamic polarization shows a decrease of porosity with the increase of film thickness, from 77.20% to 1.39% for 4.5 nm and 29.4 nm Al_2O_3 films, respectively. However, when the film thickness increases to 7.8 nm, the porosity value tends to become stable. As the film thickness further increases, the porosity decreases rather slowly. Due to the low porosity, the surface of the 7.8 nm Al_2O_3 film coated copper substrate is not severely corroded, which is confirmed by the SEM images. The method in this study can be used to measure the porosity of other insulated ultra-thin films.

Acknowledgment

The authors greatly appreciate the financial support of the National Science Fund for Distinguished Young Scholars (50825501), the Science Fund for Creative Research Groups (51321092), the National Natural Science Foundation of China (51335005), and the National Science and Technology Major Project (2008ZX02104-001). Helpful discussions with Wen Jing are gratefully acknowledged.

Notes and references

[a] *The State Key Laboratory of Tribology, Tsinghua University, Beijing 100084, China. Telephone/Fax: +86 10 6279 7362; E-mail addresses: xclu@tsinghua.edu.cn*
[b] *College of Mechanical and Electrical Engineering, China University of Petroleum, Qingdao 266580, China*

This journal is © The Royal Society of Chemistry [year]

RSC Advances Accepted Manuscript

[c] National Engineering Research Center for Nanotechnology, Shanghai 200241, China

1 S. K. Kim, G. J. Choi, S. Y. Lee, M. Seo, S. W. Lee, J. H. Han, H. S. Ahn, S. Han and C. S. Hwang, Adv. Mater., 2008, 20, 1429.
2 C. H. Chang, Y. K. Chiou, C. W. Hsu and T. B. Wu, Electrochem. Solid-State Lett., 2007, 10, G5.
3 J. Niinisto, K. Kukli, M. Heikkila, M. Ritala and M. Leskela, Adv. Eng. Mater., 2009, 11, 223.
4 C. C. Chang and F. M. Pan, J. Electrochem. Soc., 2011, 158, G97.
5 Z. Min, Z. Chenhui, L. Jianbin and L. Xinchun, Appl. Surf. Sci., 2009, 256, 322.
6 C. Casiraghi, J. Robertson and A. C. Ferrari, Mater. Today, 2007, 10, 44.
7 M. D. Groner, J. W. Elam, F. H. Fabreguette and S. M. George, Thin Solid Films, 2002, 413, 186.
8 C. C. Cheng, C. H. Chien, G. L. Luo, J. C. Liu, C. C. Kei, D. R. Liu, C. N. Hsiao, C. H. Yang and C. Y. Changa, J. Electrochem. Soc., 2008, 155, G203.
9 P. Majumder, R. Katamreddy and C. Takoudis, Electrochem. Solid-State Lett., 2007, 10, H291.
10 T. Cheon, S. H. Choi, S. H. Kim and D. H. Kang, Electrochem. Solid-State Lett., 2011, 14, D57.
11 C. Taehoon, C. Sang-Hyeok, K. Soo-Hyun and K. Dae-Hwan, Electrochem. Solid-State Lett., 2011, 14, D57.
12 S. I. Song, J. H. Lee, B. H. Choi, H. K. Lee, D. C. Shin and J. W. Lee, Surf. Coat. Technol., 2012, 211, 14.
13 R. L. Puurunen, J. Appl. Phys., 2005, 97, 121301.
14 M. Juppo, A. Rahtu, M. Ritala and M. Leskela, Langmuir, 2000, 16, 4034.
15 B. Diaz, E. Harkonen, J. Swiatowska, V. Maurice, A. Seyeux, P. Marcus and M. Ritala, Corros. Sci., 2011, 53, 2168.
16 B. Diaz, J. Swiatowska, V. Maurice, A. Seyeux, B. Normand, E. Harkonen, M. Ritala and P. Marcus, Electrochim. Acta, 2011, 56, 10516.
17 B. Diaz, E. Harkonen, V. Maurice, J. Swiatowska, A. Seyeux, M. Ritala and P. Marcus, Electrochim. Acta, 2011, 56, 9609.
18 Y. D. Zhang, D. Seghete, A. Abdulagatov, Z. Gibbs, A. Cavanagh, R. G. Yang, S. George and Y. C. Lee, *Surf. Coat. Technol.*, 2011, 205, 3334.
19 A. I. Abdulagatov, Y. Yan, J. R. Cooper, Y. Zhang, Z. M. Gibbs, A. S. Cavanagh, R. G. Yang, Y. C. Lee and S. M. George, ACS Appl. Mater. Interfaces, 2011, 3, 4593.
20 E. Harkonen, S. E. Potts, W. Kessels, B. Diaz, A. Seyeux, J. Swiatowska, V. Maurice, P. Marcus, G. Radnoczi, L. Toth, M. Kariniemi, J. Niinisto and M. Ritala, Thin Solid Films, 2013, 534, 384.
21 S. E. Potts, L. Schmalz, M. Fenker, B. Diaz, J. Swiatowska, V. Maurice, A. Seyeux, P. Marcus, G. Radnoczi, L. Toth and W. Kessels, J. Electrochem. Soc., 2011, 158, C132.
22 A. W. Ott, K. C. McCarley, J. W. Klaus, J. D. Way and S. M. George, Appl. Surf. Sci., 1996, 107, 128.
23 W. Tato and D. Landolt, J. Electrochem. Soc., 1998, 145, 4173.
24 C. Liu, Q. Bi, A. Leyland and A. Matthews, Corros. Sci., 2003, 45, 1257.
25 V. Grips, V. E. Selvi, H. C. Barshilia and K. S. Rajam, Electrochim. Acta, 2006, 51, 3461.
26 E. McCafferty, Corros. Sci., 2005, 47, 3202.
27 M. Stern and A. L. Geary, J. Electrochem. Soc., 1957, 104, 56.
28 L. Wei, X. Yimin, W. Qiming, S. Peizhen and Y. Mi, Corros. Sci., 2010, 52, 3509.
29 S. L. Shinde and K. K. Nanda, *RSC Adv.*, 2012, 2, 3647.
30 N. S. Mcintyre and M. G. Cook, *Anal. Chem.*, 1975, 47, 2208.
31 R. P. Vasquez, *Surf. Sci. Spectra*, 1993, 2, 138.
32 A. El Warraky, H. A. El Shayeb and E. M. Sherif, *Anti-Corros. Methods Mater.*, 2004, 51, 52.

RSC Advances Accepted Manuscript